KUNS-1270
HE(TH) 94/09
hep-ph/9406402

QCD S Parameter from Inhomogeneous Bethe-Salpeter Equation

Masayasu Harada[§] and Yuhsuke Yoshida[¶]

Department of Physics, Kyoto University

Kyoto 606-01, Japan

June, 1994

Abstract

We calculate the low-energy parameter S in QCD, which is also known as L_{10}, and the pion decay constant f_π using inhomogeneous Bethe-Salpeter equation in improved ladder approximation. To extract these quantities we calculate the "$V-A$" two-point function, $\Pi_{VV}(q^2)-\Pi_{AA}(q^2)$, in space-like region. We obtain $S = 0.43 \sim 0.48$, which is about 30% larger than the experimental value. The calculated f_π is well consistent with the result by solving the homogeneous Bethe-Salpeter equation for pion. We also evaluate S parameter in $SU(3)$ gauge theory with N_D doublets of fermions in connection with walking technicolor model, and find that the value of S/N_D hardly depends on N_D.

[§]Fellow of the Japan Society for the Promotion of Science for Japanese Junior Scientists.
e-mail address:harada@gauge.scphys.kyoto-u.ac.jp

[¶]e-mail address:yoshida@gauge.scphys.kyoto-u.ac.jp

1 Introduction

There is much interest to investigate the low-energy dynamics of QCD. We can see its property from the low-energy parameters of the effective Lagrangian such as L_1, L_2, ..., L_{10}, introduced by Gasser-Leutwyler[1], as well as the pion decay constant f_π. The parameter L_{10} is related to the S parameter, which expresses one of the oblique corrections[2, 3, 4] in electroweak theory.

These low-energy parameters are calculated by various models. For example the free quark model gives a half of the experimental value for QCD S parameter. It is shown that the parameter L_{10} as well as the other parameters (L_1, L_2 and L_9) are saturated by the contribution from the low-lying vector and axial-vector mesons, ρ and a_1.[5] In Ref. [6, 7], based on the nonlocal constituent-quark model, QCD S parameter is calculated using a momentum dependent quark mass function. The estimated QCD S parameter well reproduces the experimental value. In Ref. [8] they argue the corrections to the free quark loop diagram, and conclude that it is important to include the interaction which forms bound states as well as corrections to the quark propagator.

In this paper, we calculate QCD S parameter (i.e., L_{10}) using the inhomogeneous Bethe-Salpeter (BS) equation in the improved ladder approximation. The quark mass function is consistently calculated by Schwinger-Dyson (SD) equation with the same integral kernel. Our treatment here can include the effects of vector and axial-vector mesons. The QCD S parameter is given by the slope of the spin-1 part of the "$V-A$" two-point function, $\Pi_{VV}(q^2) - \Pi_{AA}(q^2)$, at $q^2 = 0$. We obtain the value $S = 0.43 \sim 0.48$. This is about 30% larger than the experimental value, $S = 0.31 \sim 0.38$ [1], which comes from the form factors of radiative pion decay $\pi \to e\nu\gamma$ and electromagnetic charge radius of pion. Noting that from first Weinberg sum rule[9] the value of this function at $q^2 = 0$ gives the pion decay constant f_π, we also calculate the value and show that it is consistent with the previous result obtained by solving the homogeneous BS equation for pion.[10] We extract the ρ meson mass and decay constant by three-pole fitting from the two-point function in the space-like region ($0 \leq -q^2 \leq (1\text{GeV})^2$).

Improved ladder approximation was first used to study the SD equations[11, 12], and well succeeded to describe the property of the chiral symmetry breaking. The homogeneous BS equation in chiral limit was solved in this approximation, which represents fundamental properties of pion.[10, 13] Especially BS equation

for pion was extensively studied in QCD and its generalized model, and the ratio between the pion decay constant f_π and the vacuum expectation value $\langle\overline{\psi}\psi\rangle$ was calculated in Ref. [10]. Moreover, the inhomogeneous BS equation in improved ladder approximation led to good predictions for low-lying meson masses.[14]

We also show the value of S parameter in other dynamical systems. We evaluate S parameter in $SU(3)$ gauge theory with $N_D(=1,\cdots,6)$ iso-spin doublets of fermions in connection with walking technicolor model[15]. Although the evaluation using dynamical mass function shows that the value of S/N_D is decreased as N_D is increased[16], we find that the value hardly depends on N_D in the improved ladder approximation.

This paper is organized as follows. In section 2, we briefly review the spectral representation of S parameter and f_π. We show how to calculate the two-point function $\Pi_{VV}-\Pi_{AA}$ from the inhomogeneous BS amplitude. Section 3 is devoted to formulations of the inhomogeneous BS equation. In section 4 we show the basic tools for the inhomogeneous BS equation and solve it numerically. Section 5 is the main part of this paper, where we show the result of the value of QCD S parameter. Further we perform three-pole fitting to the two-point function. We also investigate the walking coupling case.

2 QCD S Parameter and Two-Point Function

In this section, we define the system which we consider in this paper and summarize the basic ingredients concerning vector and axial-vector two-point functions for calculating the QCD S parameter.

Supposing that u and d quarks are massless in QCD Lagrangian, we have the chiral $SU(2)_L\times SU(2)_R$ symmetry. As is well known, this symmetry is spontaneously broken down to its subgroup $SU(2)_V$, and massless pions appear. Chiral Lagrangian well represents the symmetrical aspects of the interaction among pions and external currents which couple to photon, W and Z bosons. There are several low-energy parameters in the effective chiral Lagrangian and these parameters are to be determined from the dynamics of QCD.

For calculating QCD S parameter we consider the vector and axial-vector current

defined by

$$\left\{ \begin{array}{l} V_\mu^a(x) = \overline{\psi}(x)\dfrac{\tau^a}{2}\gamma_\mu\psi(x) \ , \\ A_\mu^a(x) = \overline{\psi}(x)\dfrac{\tau^a}{2}\gamma_\mu\gamma_5\psi(x) \ , \end{array} \right. \qquad \psi = \left(\begin{array}{c} u \\ d \end{array} \right) \ , \tag{2.1}$$

where τ^a $(a = 1, 2, 3)$ is Pauli matrix. Then we define the two-point function Π_{JJ} $(J = V, A)$

$$\begin{aligned} \delta^{ab}\Pi_{JJ}(q^2) &\equiv \epsilon^\mu\epsilon^\nu i\int d^4x\, e^{iqx}\,\langle 0|\,\mathrm{T}J_\mu^a(x)J_\nu^b(0)\,|0\rangle \ , \\ J_\mu^a(x) &\equiv V_\mu^a(x)\,,\ A_\mu^a(x)\ , \end{aligned} \tag{2.2}$$

where a, b are iso-spin indices, ϵ_μ is the polarization vector defined by $\epsilon\cdot q = 0$, $\epsilon\cdot\epsilon = -1$.

The QCD S parameter and the pion decay constant are given by the two-point function of "$V - A$" type:

$$S = 4\pi\,\frac{d}{dq^2}\left[\Pi_{VV}(q^2) - \Pi_{AA}(q^2)\right]\Big|_{q^2=0} \ , \tag{2.3}$$

$$f_\pi^2 = \Pi_{VV}(0) - \Pi_{AA}(0) \ . \tag{2.4}$$

QCD S parameter is related to the Gasser-Leutwyler parameter L_{10} as $S = -16\pi L_{10}$.

Using spectral representation of vector and axial-vector currents, eqs. (2.3) and (2.4) are rewritten into

$$S = 4\pi\int_0^\infty \frac{ds}{s^2}\,\left[\rho_{_V}(s) - \rho_{_A}(s)\right] \ , \tag{2.5}$$

$$f_\pi^2 = \int_0^\infty \frac{ds}{s}\,\left[\rho_{_V}(s) - \rho_{_A}(s)\right] \ , \tag{2.6}$$

where $\rho_{_V}(s)$ and $\rho_{_A}(s)$ are the spin-1 parts of the vector and axial-vector spectral functions, respectively. Equations (2.5) and (2.6) are referred to as the Das-Mathur-Okubo sum rule[17] and the first Weinberg sum rule[9], respectively. We can easily understand the above equations by the following way: The commutator of the conserved current $J_\mu^a(x)$ is decomposed into

$$\begin{aligned} \langle 0|\left[J_\mu^a(x), J_\nu^b(0)\right]|0\rangle &= -\delta^{ab}\int_0^\infty \frac{ds}{s}\,\rho_{_J}(s)(sg_{\mu\nu} + \partial_\mu\partial_\nu)\Delta(x;s) \\ &\quad -\delta^{ab}\,\rho^{(0)}\,\partial_\mu\partial_\nu\Delta(x;0) \ , \\ \Delta(x;s) &= \int\frac{d^4q}{(2\pi)^3}e^{-iqx}\epsilon(q_0)\delta(s-q^2) \ , \end{aligned} \tag{2.7}$$

where $\rho^{(0)}$ denotes a contribution from massless scalar particle. Noting that massless pion couples to the axial-vector current A^a_μ while no massless particle couples to the vector current V^a_μ, we find $\rho^{(0)}_A = f_\pi^2$ and $\rho^{(0)}_V = 0$. The "$V-A$" two-point function can be expressed as

$$\begin{aligned} & i\int d^4x\, e^{iqx}\Big\langle 0\Big|\mathrm{T}\left[V^a_\mu(x)V^b_\nu(0) - A^a_\mu(x)A^b_\nu(0)\right]\Big|0\Big\rangle \\ &= \; -\delta^{ab}\int_0^\infty \frac{ds}{s}\,\frac{\rho_V(s)-\rho_A(s)}{s-q^2-i\epsilon}(sg_{\mu\nu}-q_\mu q_\nu) + \delta^{ab}\,\frac{q_\mu q_\nu}{q^2}\,f_\pi^2\ . \end{aligned} \tag{2.8}$$

Thus, we obtain eqs. (2.5) and (2.6) using eqs. (2.3) and (2.4).

Let us consider the following three-point vertex function

$$\begin{aligned} \delta^j_i\ \left(\frac{\tau^a}{2}\right)_f^{f'}\int\frac{d^4p}{(2\pi)^4}\,e^{-ipr}\,\chi_{\alpha\beta}(p;q,\epsilon) \quad = \\ \epsilon^\mu\ \int d^4x\ e^{iqx}\ \Big\langle 0\Big|\mathrm{T}\,\psi_{\alpha i f}(r/2)\,\overline{\psi}^{jf'}_\beta(-r/2)\,J^a_\mu(x)\Big|0\Big\rangle\ , \end{aligned} \tag{2.9}$$

where $\chi\ (=\chi_V, \chi_A)$ is bi-spinor, which we call inhomogeneous BS amplitude. Here $(f,\ f',\ \cdots)$, $(i,\ j,\ \cdots)$ and $(\alpha,\ \beta,\ \cdots)$ denote flavor, color and spinor indices, respectively. This inhomogeneous BS amplitude has definite spin, parity and charge conjugation, i.e., $J^{PC} = 1^{--}$ for vector case and 1^{++} for axial-vector case.

Closing the fermion legs of the three-point function, we find that the two-point function is expressed in terms of the inhomogeneous BS amplitude χ:

$$\begin{aligned} \Pi_{JJ}(q^2) &= -\frac{1}{3}\sum_\epsilon\int\frac{d^4p}{i(2\pi)^4}\,\frac{N_c}{2}\,\mathrm{tr}\Big[(\epsilon\cdot G)\,\chi(p;q,\epsilon)\Big]\ , \\ G_\mu &= \begin{cases} \gamma_\mu & \text{for vector vertex} \\ \gamma_\mu\gamma_5 & \text{for axial-vector vertex} \end{cases}\ , \end{aligned} \tag{2.10}$$

where $N_c \equiv 3$ is the number of $SU(3)_c$ color and we average over the polarizations for convenience; $\Pi_{JJ}(q^2)$ in eq. (2.2) does not depend on the polarization ϵ_μ. Although the vector or axial-vector two-point function itself is logarithmically divergent, the chiral symmetry guarantees the finiteness of the quantity $\Pi_{VV}(q^2) - \Pi_{AA}(q^2)$. The divergences appearing in each two-point function cancel because the structures of the divergences are exactly the same.[18]

The quantities we should first calculate are vector and axial-vector inhomogeneous BS amplitudes χ_V and χ_A, which are finite by current conservation. Then, we perform the momentum integration after taking the difference to obtain the "$V-A$"

two-point function, i.e.,

$$\Pi_{VV}(q^2)-\Pi_{AA}(q^2) = -\frac{1}{3}\sum_{\epsilon}\int \frac{d^4p}{i(2\pi)^4}\,\frac{N_c}{2}\,\mathrm{tr}\Big[\,\not{\epsilon}\chi_V(p;q,\epsilon) - \not{\epsilon}\gamma_5\chi_A(p;q,\epsilon)\,\Big]\ . \quad (2.11)$$

This integration converges as we mentioned above. In this paper, we work with the space-like total momentum q_μ ($q_E^2 \equiv -q^2 > 0$), then we do not encounter the singularities which come from meson poles in time-like region.

3 Inhomogeneous Bethe-Salpeter Equation

In this section, we discuss the basic formulations for solving the vector and axial-vector inhomogeneous BS equations. SD equation is solved by the same BS kernel. We give the component form of the inhomogeneous BS equation. The inhomogeneous BS equations are solved in the space-like region for the total momentum q_μ, $q_E^2 > 0$.

In the non-perturbative treatment of QCD by BS approach, the most important quantity is the BS kernel which expresses the QCD interaction by the gluon. In the improved ladder approximation with Landau gauge, the BS kernel K is defined by [the momentum assignment is chosen as shown in Fig. 1]

$$K(p,k) = C_2\, g^2(p,k)\frac{1}{-(p-k)^2}\left(g_{\mu\nu} - \frac{(p-k)_\mu(p-k)_\nu}{(p-k)^2}\right)\gamma^\mu\otimes\gamma^\nu\ , \quad (3.1)$$

where $C_2 \equiv (N_c^2-1)/(2N_c)$ is the second Casimir of $SU(3)_c$ color fundamental

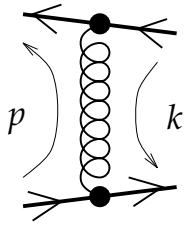

Figure 1: The Feynman diagram of the BS kernel $K(p,k)$ in eq. (3.1) which we use in our calculation. The helix denotes the gluon propagator intermediating between two quarks.

representation and we use the tensor product notation[19]

$$(A\otimes B)\chi \equiv A\chi B\ . \quad (3.2)$$

In the BS kernel (3.1) we adopt the Higashijima-Miransky approximation[11, 12] for the running coupling, $g^2(p,k) = g^2(\max(-p^2,-k^2))$. This running coupling allows us to include the property of asymptotic freedom of QCD. Using this running coupling the chiral symmetry is always spontaneously broken. The detailed structure of the running coupling is given in section 4.1.

For solving the inhomogeneous BS equation, we need the full quark propagator $S_F(p)$, which is given by solving the SD equation with the *same* BS kernel for preserving the chiral symmetry. The wave function renormalization factor of quark propagator is one in Landau gauge in the Higashijima-Miransky approximation. Then the quark mass function $\Sigma(p)$ is given by

$$i\Sigma(p) = K * S_F(p) \ , \tag{3.3}$$

where

$$S_F(p) = \frac{i}{\not{p} - \Sigma(p)} \ . \tag{3.4}$$

The operator "$*$" acting on the BS kernel K and a bi-spinor Ψ denotes momentum integration:

$$K * \Psi(p) \equiv \int \frac{d^4k}{i(2\pi)^4} \ K(p,k) \ \Psi(k) \ . \tag{3.5}$$

Now, the inhomogeneous BS equation for $\chi(p;q,\epsilon)$ is

$$(T - K*) \ \chi = (\epsilon \cdot G) \ , \qquad (\ G_\mu = \gamma_\mu, \gamma_\mu\gamma_5 \ ) \tag{3.6}$$

where

$$T = T(p;q) \equiv S_F^{-1}(p + \frac{q}{2}) \otimes S_F^{-1}(p - \frac{q}{2}) \ . \tag{3.7}$$

The formal solution is given by

$$\chi = \frac{1}{T - K*} \ (\epsilon \cdot G) \ . \tag{3.8}$$

This solution can be reinterpreted by expanding it into the power series of the BS kernel as (see Fig.2)

$$\chi = T^{-1}(\epsilon \cdot G) + T^{-1}K * T^{-1}(\epsilon \cdot G) + T^{-1}\left(K * T^{-1}\right)^2 (\epsilon \cdot G) + \cdots \ . \tag{3.9}$$

We can expand the inhomogeneous BS amplitude $\chi = \chi_V, \ \chi_A$ into eight invariant amplitudes:

$$\chi_J(p;q,\epsilon) = \sum_{i=1}^{8} \Gamma_i^{(J)}(p;q,\epsilon) \ \chi_J^i(p;q) \ , \qquad (\ J = V, A \ ) \tag{3.10}$$

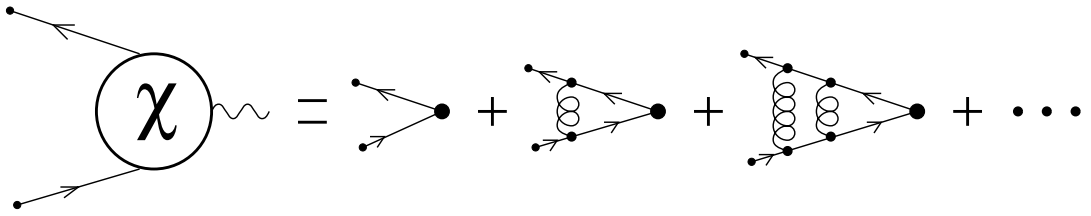

Figure 2: The expansion of vector or axial-vector inhomogeneous BS amplitude given in eq. (3.9).

where χ_J^i $(i = 1, \cdots, 8)$ is scalar quantity. $\Gamma_i^{(J)}$ is the vector or axial-vector base defined by

$$\begin{aligned}
&\Gamma_1^{(V)} = \not{\epsilon}, \qquad \Gamma_2^{(V)} = \tfrac{1}{2}[\not{\epsilon}, \not{p}](p \cdot \widehat{q}), \quad \Gamma_3^{(V)} = \tfrac{1}{2}[\not{\epsilon}, \not{\widehat{q}}], \qquad \Gamma_4^{(V)} = \tfrac{1}{3!}[\not{\epsilon}, \not{p}, \not{\widehat{q}}], \\
&\Gamma_5^{(V)} = (\epsilon \cdot p), \quad \Gamma_6^{(V)} = \not{p}(\epsilon \cdot p), \qquad \Gamma_7^{(V)} = \not{\widehat{q}}(p \cdot \widehat{q})(\epsilon \cdot p), \quad \Gamma_8^{(V)} = \tfrac{1}{2}[\not{p}, \not{\widehat{q}}](\epsilon \cdot p),
\end{aligned} \tag{3.11}$$

and

$$\Gamma_i^{(A)} = \Gamma_i^{(V)} \gamma_5 \ , \tag{3.12}$$

where $\widehat{q}_\mu = q_\mu / \sqrt{q_E^2}$ and $[a, b, c] \equiv a[b, c] + b[c, a] + c[a, b]$. We note that the dependence on the polarization vector ϵ_μ is isolated in the base $\Gamma_i^{(J)}(p; q, \epsilon)$.

To solve the integral equation (3.6) numerically, we perform the Wick rotation on the momentum k integration and analytic continuation on the relative momentum p as usual. We introduce the scalar variables u, x, v and y as

$$\begin{aligned}
&p \cdot \widehat{q} = -u, \quad p^2 = -u^2 - x^2, \\
&k \cdot \widehat{q} = -v, \quad k^2 = -v^2 - y^2 \ .
\end{aligned} \tag{3.13}$$

Multiplying eq. (3.6) by the Dirac conjugate base $\overline{\Gamma}_i$, taking the trace and summing over the polarization, we convert it into the component form[¶]

$$\sum_j \ (T_{ij} - K_{ij} \star) \, \chi^j = I_i \ , \tag{3.14}$$

where

$$I_i(u, x) \ = \ \frac{1}{4} \sum_\epsilon \mathrm{tr} \left[\ \overline{\Gamma}_i(p; \widehat{q}, \epsilon) \, (\epsilon \cdot G) \ \right] \ ,$$

[¶]We evaluate the matrix elements of $T_{ij}(u, x)$ and $K_{ij}(u, x; v, y)$ by an algebraic calculation program.

$$
\begin{aligned}
T_{ij}(u,x) &= \frac{1}{4}\sum_{\epsilon} \mathrm{tr}\left[\, \overline{\Gamma}_i(p;\widehat{q},\epsilon)\, T(p;q)\, \Gamma_j(p;\widehat{q},\epsilon)\,\right] \ , \\
K_{ij}(u,x;v,y) &= 2\pi \int_{-1}^{1} d\cos\theta\, \frac{1}{4}\sum_{\epsilon} \mathrm{tr}\left[\, \overline{\Gamma}_i(p;\widehat{q},\epsilon)\, K(p,k)\, \Gamma_j(k;\widehat{q},\epsilon)\,\right] \ . \qquad (3.15)
\end{aligned}
$$

Here θ is the angle between the 3-vector part of p and k; $\cos\theta \equiv \boldsymbol{p}\cdot\boldsymbol{k}/|\boldsymbol{p}||\boldsymbol{k}|$. The operation $\star$ denotes u and x integrations, i.e., $2\pi\int_{-1}^{1} d\cos\theta \star \equiv *$. We should note that the Dirac conjugation is taken to be

$$
\overline{\chi}(p;q,\epsilon) \equiv \gamma_0 \chi(p^*;q^*,\epsilon)^\dagger \gamma_0 \ . \qquad (3.16)
$$

The complex conjugate on p and q should be taken to preserve Feynman causality of inhomogeneous BS amplitudes when those momenta become complex by analytic continuation.[19] Our choice of the bases (3.11) and (3.12) leads to the fact that the matrix K_{ij} is independent of q_E^2. [The q_E^2 dependence of χ^j comes from T_{ij} only.]

It should be noticed that the invariant amplitude χ^i is even function of $(p\cdot\widehat{q})$. Namely it is regarded as an even function of u with an arbitrary constant q_E^2:

$$
\chi^i(u,x) = \chi^i(-u,x) \ . \qquad (3.17)
$$

This is the result of the charge conjugation property

$$
\begin{aligned}
C\chi(-p;q,\epsilon)^T C^{-1} &= -\chi(p;q,\epsilon) \ , \\
C\Gamma_i(-p;q,\epsilon)^T C^{-1} &= -\Gamma_i(p;q,\epsilon) \ ,
\end{aligned} \qquad (3.18)
$$

where $C = i\gamma_0\gamma_2$ is charge conjugation matrix. Similarly from this property, one can easily check that T and K are real definite and symmetric matrices:

$$
\begin{aligned}
T_{ij}(u,x) &= T_{ji}(u,x) \ , \\
K_{ij}(u,x;v,y) &= K_{ji}(v,y;u,x) \ . \qquad (3.19)
\end{aligned}
$$

This is an important property, from which we find that the inhomogeneous BS amplitudes are real definite, and thus the two-point function is real definite.

4 Numerical Calculations

In this section we give the detailed form of the running coupling. We calculate the quark mass function and the inhomogeneous BS amplitudes. In the following, all the dimensionful parameters are rescaled by Λ_{QCD}, otherwise stated.

4.1 Running Coupling

Running coupling $g^2(\mu^2)$ can be well approximated by the result from one-loop β-function in high energy region, so we basically use it in the BS kernel (3.1). However the one-loop running coupling blows up at $\mu = \Lambda_{\rm QCD}$ and we have no idea about the functional form in low energy region. One prescription is to adopt the Higashijima approximation[11] in which $g^2(\mu^2)$ is constant below some scale and is one-loop running coupling above that scale. It is important that the running coupling and its derivative are continuous with respect to $\ln\mu^2$, otherwise the derivative of the mass function is discontinuous.[†] We achieve this continuities by interpolating between one-loop running coupling and a fixed value with the second order polynomial of $\ln\mu^2$. According to Ref. [10], we adopt the following functional form of the running coupling:

$$\alpha(\mu^2) \equiv \frac{g^2(\mu^2)}{4\pi} = \alpha_0 \times \begin{cases} \dfrac{1}{t} & \text{if } t_F < t \\ \dfrac{1}{t_F} + \dfrac{(t_F - t_C)^2 - (t - t_C)^2}{2t_F^2(t_F - t_C)} & \text{if } t_C < t < t_F \\ \dfrac{1}{t_F} + \dfrac{(t_F - t_C)^2}{2t_F^2(t_F - t_C)} & \text{if } t < t_C \end{cases} , \quad (4.1)$$

where $t = \ln\mu^2$ and $\alpha_0 = 12\pi/(11N_c - 2N_f)$ with N_f being the number of flavors. As seen in Fig. 3, the support of the "$V - A$" two-point function lies below in the threshold of c quark, so we take $N_f = 3$ and $\alpha_0 = 4\pi/9$. We take the same parameter choice as in Ref. [14], i.e., $t_F = 0.5$ and $t_C = -2.0$. It is observed at least that the specific choice of the parameter t_F does not affect the "physical" quantity $\langle\overline{\psi}\psi\rangle$.[10] We will check the dependence on the infrared cutoff t_F of the QCD S parameter in the section 5.

4.2 Mass Function

Before solving the inhomogeneous BS equation, we have to calculate the mass function of quarks. The SD equation (3.3) reads

$$\Sigma(x) = \frac{3C_2}{4\pi}\int_0^\infty dy\, \frac{\alpha(\max(x,y))}{\max(x,y)}\, \frac{y\Sigma(y)}{y + \Sigma^2(y)} \quad (4.2)$$

in the Higashijima-Miransky approximation, where $x = -p^2$ and $y = -k^2$. This integral equation is solved by the following way: First, we discretize the equation

[†]We easily find this point if we convert the SD equation into differential equation.

fine enough. Second, starting from the functional form $\Sigma(x) = \text{constant} \neq 0$, we iteratively update the mass function according to eq. (4.2) itself until the functional form converges.

When we solve the inhomogeneous BS equation, we need the mass function at the momenta $p \pm q/2$. To obtain the mass function $\Sigma(-(p \pm q/2)^2)$, we substitute the above convergent mass function $\Sigma(y)$ into RHS of eq. (4.2) after putting $x = -(p \pm q/2)^2$, and carry out the y integration. We note that we can independently choose the lattice points for solving the SD and inhomogeneous BS equations.

4.3 Inhomogeneous BS Amplitude

Let us consider the inhomogeneous BS equation (3.14). We discretize it and solve the resulting linear equation numerically. Here, we should note that $\chi^j(v, y)$ is even function of v. Then we restrict the integral region over variable v to be positive, $v > 0$, after replacing the kernel as

$$K_{ij}(u, x; v, y) \to K_{ij}(u, x; v, y) + K_{ij}(u, x; -v, y) \ . \tag{4.3}$$

The fundamental variables used to solve the inhomogeneous BS equation (3.14) are U and X defined by

$$u = \exp U \ , \quad x = \exp X \quad . \tag{4.4}$$

As for the strong interaction, it is important to take into account interactions around $\Lambda_{\rm QCD}$ scale rather than that in the high energy scale. The above choice (4.4) is suitable for our calculation. We discretize the variables U and X at $N_{BS} = 22$ points evenly spaced in the intervals

$$\begin{aligned} U &\in [\ \lambda_U\ ,\ \Lambda_U\ ] = [\ -5.5\ ,\ 2.5\ ] \ , \\ X &\in [\ \lambda_X\ ,\ \Lambda_X\ ] = [\ -2.5\ ,\ 2.5\ ] \ . \end{aligned} \tag{4.5}$$

In numerical integration, to avoid integrable logarithmic singularity at $(u, x) = (v, y)$, we take four-point average[14] of the BS kernel $K_{ij}(u, x; v, y)$ as

$$\begin{aligned} K_{ij}(u, x; v, y) \ \to \ & \frac{1}{4}\,[\ K_{ij}(u, x; v_+, y_+) \ + \ K_{ij}(u, x; v_+, y_-) \ + \\ & K_{ij}(u, x; v_-, y_+) \ + \ K_{ij}(u, x; v_-, y_-)\ ] \ , \end{aligned} \tag{4.6}$$

where

$$v_\pm = \exp(V \pm \frac{1}{4} D_U) \ , \quad D_U = (\Lambda_U - \lambda_U)/(N_{BS} - 1) \ ,$$
$$y_\pm = \exp(Y \pm \frac{1}{4} D_X) \ , \quad D_X = (\Lambda_X - \lambda_X)/(N_{BS} - 1) \ . \tag{4.7}$$

Now, we solve the inhomogeneous BS equations for the vector and the axial-vector currents separately, so that we obtain the amplitudes $\chi_V(u,x)$ and $\chi_A(u,x)$. We use FORTRAN subroutine package for these numerical calculations.

5 Results

In this section, first we calculate the spin-1 part of the two-point function, $\Pi_{VV}(q^2) - \Pi_{AA}(q^2)$, then extract the QCD S parameter and the pion decay constant f_π.

5.1 QCD S Parameter

After obtaining the vector and axial-vector inhomogeneous BS amplitudes, $\chi_V(u,x)$ and $\chi_A(u,x)$, numerically, we calculate the "$V-A$" two-point function using eq. (2.11).

The QCD S parameter and the pion decay constant are calculated from the formulae (2.3) and (2.4). Using the numerical differentiation formula, we extract S from four data points of $\Pi_{VV} - \Pi_{AA}$ at $q_E^2 \equiv -q^2 = 0.0, 0.2, 0.4, 0.6$. In this choice of the interval of q_E^2, $h = 0.2$, the error of numerical differentiation is estimated as $O(h^3) \sim 0.8\%$.[¶] On the other hand, the fluctuation δ of the value of $\Pi_{VV} - \Pi_{AA}$, which comes from the dependence on the lattice size, causes the error $O(\delta/h)$ of S. As we will show below, choosing large lattice size allows us to make the fluctuation δ within 1%. Then the error of S is expected as $O(\delta/h) \sim 5\%$. When we take larger interval h, the error of numerical differentiation becomes large. On the other hand, the fluctuation of S, $O(\delta/h)$, is enhanced by taking the smaller interval h. We have checked the validity of the differentiation for several choices of h and for various numerical differentiation formulae.

In what follows we investigate all the dependences on the parameters, i.e., the momentum cutoff (4.5), the lattice size N_{BS} and the infrared cutoff t_F of the running coupling.

[¶] It is natural to estimate the numerical error with the dimensionless quantities scaled by $\Lambda_{\rm QCD}$.

First, we check the dependence on the infrared and ultraviolet cutoff in eq. (4.5). The typical example of the support of the "$V-A$" two-point function is shown in Fig. 3 with $q^2 = 0$, $t_F = 0.5$ and $N_{BS} = 22$. The choice (4.5) covers the dominant support very well. Further, the position of the support does not change if we vary the values of q^2, t_F and N_{BS}. There is a slight rise in the high energy region, which originates in the numerical error of the cancellation of divergences between Π_{VV} and Π_{AA}. This error, if any, affects the two-point function with 1% at most.

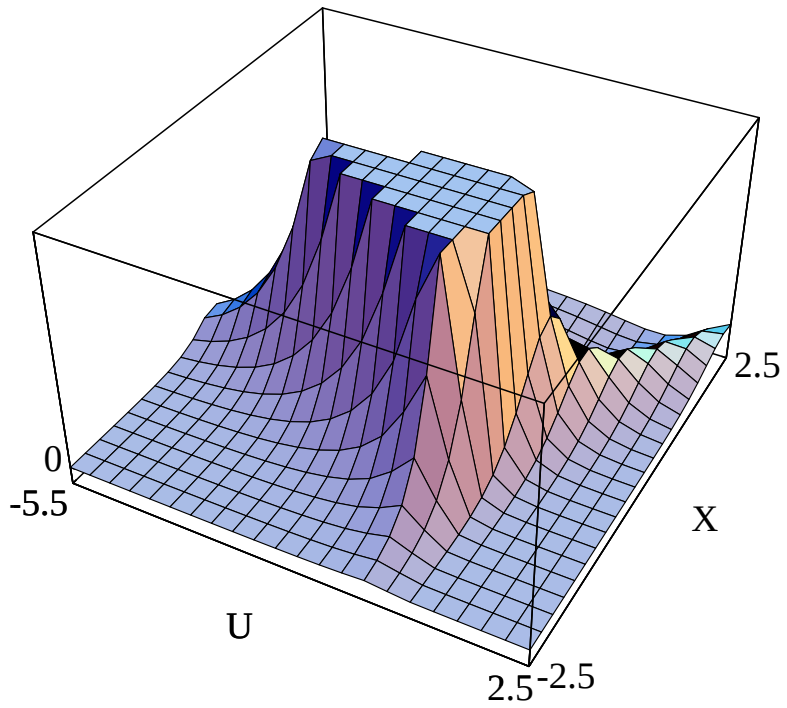

Figure 3: The support of "$V-A$" two-point function. The upper 9/10 of the figure is cripped.

Second, we check the dependence on the lattice size N_{BS}. We show the values of the QCD S parameter and the pion decay constant f_π for several values of N_{BS} in Table 1. We also show the values of $\Lambda_{\rm QCD}$ which are fixed by imposing $f_\pi = 93$ MeV. Even in $N_{BS} = 14$ the fluctuation δ of f_π^2 is within 1% and the fluctuation of S is several percents. So, it is enough to take $N_{BS} = 22$.

Third, we check the dependence on the infrared cutoff t_F taking $N_{BS} = 22$. We show the values of the QCD S parameter and the pion decay constant f_π with

N_{BS}	10	12	14	16	18	20	22
S	0.500	0.388	0.452	0.481	0.455	0.474	0.464
$(f_\pi/\Lambda_{\rm QCD})^2 \times 100$	3.71	3.76	3.95	4.04	4.04	4.06	4.05
$\Lambda_{\rm QCD}$ [MeV]	483	479	468	462	463	461	462

Table 1: N_{BS} dependence of the value of the QCD S parameter and $f_\pi/\Lambda_{\rm QCD}$. We also show the values of $\Lambda_{\rm QCD}$ calculated by imposing $f_\pi = 93$ MeV. We take the parameter choice $t_F = 0.5$.

several values of t_F in Table 2. The variations of S are within 10%. We also calculate the scale $\Lambda_{\rm QCD}$ by imposing $f_\pi = 93$ MeV, and the results are shown in Table 2. The values of $\Lambda_{\rm QCD}$ are consistent with the results in Ref. [10] which are calculated from the homogeneous BS amplitude of pion with the same BS kernel as ours. For example, their typical value is $\Lambda_{\rm QCD} = 484$ MeV with $t_F = 0.5$. [Our t_F corresponds to t_{IF} in Ref. [10] as $t_F = 1 + t_{IF}$.]

t_F	0.3	0.5	0.7	0.9	1.1
S	0.432	0.464	0.478	0.481	0.470
$(f_\pi/\Lambda_{\rm QCD})^2 \times 100$	3.43	4.05	4.10	3.75	3.12
$\Lambda_{\rm QCD}$ [MeV]	502	462	459	481	526

Table 2: t_F dependence of the value of the QCD S parameter and $f_\pi/\Lambda_{\rm QCD}$. We also show the values of $\Lambda_{\rm QCD}$ calculated by imposing $f_\pi = 93$ MeV. We fix the lattice size as $N_{BS} = 22$.

We show the value of the QCD S parameter which are the main results of this paper:

$$S = 0.43 \sim 0.48 \ . \tag{5.1}$$

Let us consider what effects are included by our approach. The lowest contribution to QCD S parameter is given by one-loop quark diagram shown in Fig. 4(a). There are two classes of the higher order corrections to this diagram, i.e., corrections to the quark propagator and binding forces to form $q\overline{q}$ bound state. [Effects of gluon condensation[20] are not considered here.] These are schematically expressed by the diagrams in Figs. 4(b) and 4(c). The improved ladder approximation includes these

two corrections simultaneously.

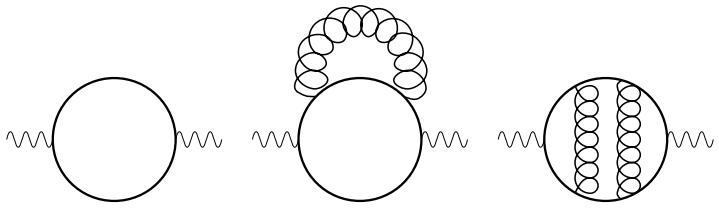

Figure 4: The schematic view of the Feynman diagrams contributing to the "$V-A$" two-point function, $\Pi(q_E^2) \equiv \Pi_{VV}(q_E^2) - \Pi_{AA}(q_E^2)$. (a) is quark one-loop diagram, (b) expresses inclusion of momentum dependent mass function, (c) represents binding forces to form quark-antiquark bound state.

QCD S parameters

Our value	GL	VMD	LCQ	NCQM	FQL
$0.43 \sim 0.48$	0.342 ± 0.034	0.37	0.21	$0.30 \sim 0.40$	0.16

Table 3: The predictions of QCD S parameter in various models. GL : experimental value by Gasser-Leutwyler, VMD : vector and axial-vector dominance model, LCQ : local chiral quark model, NCQM : nonlocal constituent-quark model. We also show the value calculated by free quark one-loop diagram (FQL), $S = N_c/(6\pi)$.

Now, let us compare our result with the experimental value (GL)[1] and other predictions from the vector meson dominance model (VMD)[5], the local chiral quark model (LCQ)[8], and the nonlocal constituent-quark model (NCQM)[6, 7]. We show their results in Table 3.[¶] The FQL or LCQ model gives a half of the experimental

[¶] They calculate $L_{10}(\mu)$ at the renormalization scale $\mu = m_\eta$ (LCQ, NCQM) or $\mu = m_\rho$ (VMD). Following Ref. [1, 8], we convert their values of $L_{10}(\mu)$ to S by

$$S = -16\pi \left[L_{10}(\mu) + \frac{1}{192\pi^2} \left(\ln \frac{m_\pi^2}{\mu^2} + 1 \right) \right] .$$

value (GL) of S. We should include higher order corrections as in Figs. 4(b) and 4(c). The VMD model well reproduces the experimental value of S. This implies that it is important to include the contribution from the bound state, in other words, we should take into account the binding force as in Fig. 4(c). On the other hand, in NCQM model the value of QCD S parameter is improved by the inclusion of the momentum dependent mass function as in Fig. 4(b). The high energy behavior of this diagram is consistent with the result by operator product expansion (OPE).[21] For these reasons we include these two corrections by the improved ladder approximation. Our value of QCD S parameter is 30% larger than the experimental value. For one thing further corrections beyond the improved ladder approximation may be needed (e.g., the decay widths of vector or axial-vector mesons are not taken into account in our approximation); for another the difference between our value and the experimental one may be caused by the slight breaking of the chiral Ward-Takahashi (WT) identity. Reference [22] suggests that if we use the ladder approximation completely consistent with WT identity we could make up the difference.¶

5.2 Pole Fitting

We extract the mass m_ρ and the decay constant f_ρ of ρ meson by three-pole fitting:

$$\Pi(q_E^2) = \frac{f_\rho^2 m_\rho^2}{q_E^2 + m_\rho^2} - \frac{f_{R_1}^2 m_{R_1}^2}{q_E^2 + m_{R_1}^2} + \frac{f_{R_2}^2 m_{R_2}^2}{q_E^2 + m_{R_2}^2} \ , \tag{5.2}$$

from the two-point function $\Pi(q_E^2) \equiv \Pi_{VV}(q_E^2) - \Pi_{AA}(q_E^2)$ in space-like region ($0 \leq q_E^2 \leq (1\text{GeV})^2$) with $t_F = 0.5$. The positive sign contribution in eq. (5.2) comes from the two-point function of the vector current and the negative sign contribution from that of the axial-vector current. The last two terms represent the contributions from other mesons heavier than ρ meson. The decay constant of ρ meson in eq. (5.2) is defined by

$$\left\langle 0 \middle| V_\mu^a(0) \middle| \rho^b(q,\epsilon) \right\rangle = \delta^{ab} \epsilon_\mu f_\rho m_\rho \ . \tag{5.3}$$

We show our two-point function $\Pi(q_E^2)$ and the best fitting curve in Fig.5. The best fitted values are shown in Table 4. These values should be compared with those

¶ There is 20% difference in the value of f_π between the "consistent" ladder approximation and Pagels-Stokar formula[22], while Pagels-Stokar formula and the improved ladder approximation give almost the same value of f_π[14]. [We note that the different BS kernels are used in two references. For details see Refs. [14, 22].]

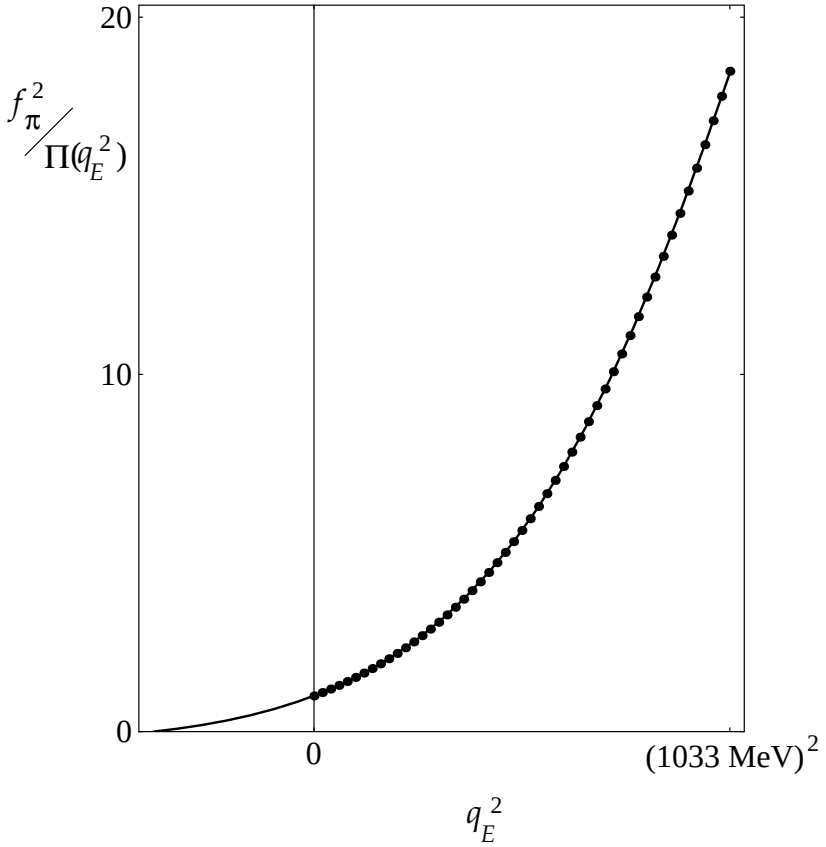

Figure 5: Three pole fitting of our two-point function, $\Pi(q_E^2) = \Pi_{VV}(q_E^2) - \Pi_{AA}(q_E^2)$. The solid line is the best fitting curve, the dots denote the value of our $\Pi(q_E^2)$.

	Our value	Experiment [23]
f_ρ [MeV]	133	144 ± 8
m_ρ [MeV]	643	768

Table 4: The best fitted values of the mass and decay constant of ρ meson. We use our value of Λ_{QCD} ($= 462$ [MeV]).

in Ref. [14]. Because we need no further regularization in calculating the "$V-A$" two-point function, we do not have to introduce cutoff parameter as in Ref. [14].

We find that the sum of the pole residues $f_\rho^2 m_\rho^2 - f_{R_1}^2 m_{R_1}^2 + f_{R_2}^2 m_{R_2}^2$ vanishes, which implies that our $\Pi(q_E^2)$ behaves as $1/q_E^4$. The result from the improved ladder approximation reproduces the high energy behavior of the "$V-A$" two-point function required by that from OPE in QCD. This means that the spectral functions of our $\Pi(q_E^2)$ in eq. (2.8) satisfies the second Weinberg sum rule:

$$\int_0^\infty ds\,[\rho_V(s) - \rho_A(s)] = 0\ . \tag{5.4}$$

The masses and decay constants of the heavier mesons are unstable for fitting; we obtain several best fitted curves with different values for the masses and decay constants of the heavier mesons, although they satisfy the first and second Weinberg sum rules. On the other hand, the lowest meson mass and decay constant are very stable.

We compare our two-point function with that from the ρ and a_1 meson dominance model. In this model the first and second Weinberg sum rules read

$$f_\rho^2 - f_{a_1}^2 = f_\pi^2\ , \qquad f_\rho^2 m_\rho^2 - f_{a_1}^2 m_{a_1}^2 = 0\ . \tag{5.5}$$

It is convenient to adopt the following parameterization:

$$f_\rho = f_\pi \cosh\theta\ , \quad f_{a_1} = f_\pi \sinh\theta\ . \tag{5.6}$$

Then the resultant "$V-A$" two-point function $F(q_E^2)$ is expressed by

$$F(q_E^2) = f_\pi^2\ \frac{m_\rho^4 \coth^2\theta}{(q_E^2 + m_\rho^2)(q_E^2 + m_\rho^2 \coth^2\theta)}\ . \tag{5.7}$$

We show the function $F(q_E^2)$ for two different choices of m_ρ and $\coth\theta$ in Fig. 6 with our $\Pi(q_E^2)$. Taking $(\coth\theta, m_\rho) = (1, 643\ [\mathrm{MeV}])$ makes $F(q_E^2)$ well agree with our $\Pi(q_E^2)$. However, when we use the experimental value $(f_\rho, m_\rho) = (144, 768)[\mathrm{MeV}]$, $F(q_E^2)$ does not match with our $\Pi(q_E^2)$.

5.3 Walking Coupling Case

We apply the method for inhomogeneous BS equation to the other dynamical system than QCD, i.e., $SU(3)$ gauge theory with N_D doublets of massless fermions.

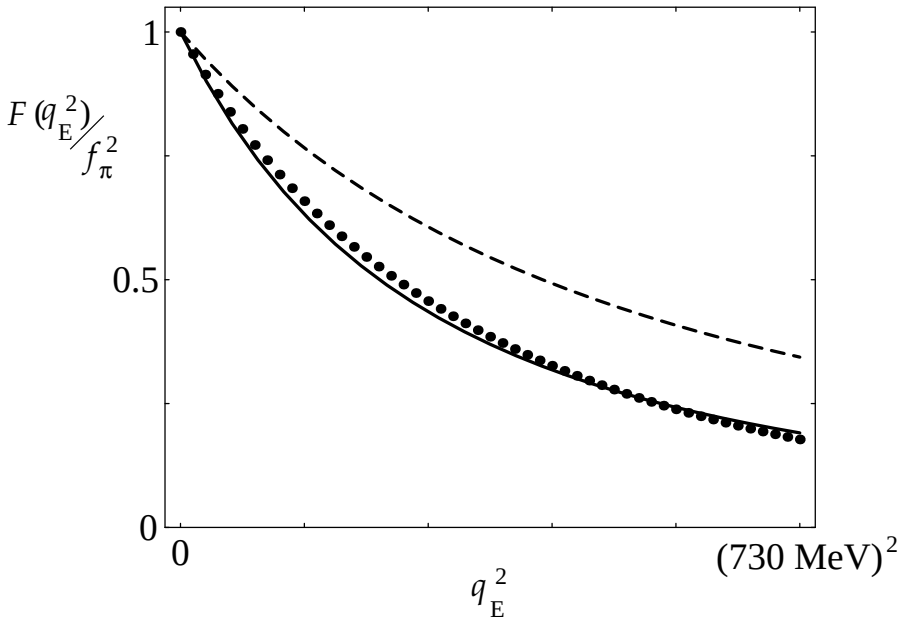

Figure 6: The comparison with the ρ and a_1 meson dominance model. The solid line denotes $F(q_E^2)$ with $(\coth\theta, m_\rho) = (1, 643\ [\mathrm{MeV}])$, the broken line, $F(q_E^2)$ with $(f_\rho, m_\rho) = (144, 768)$ [MeV]. The dots denote the values of our $\Pi(q_E^2)$.

The difference between the real QCD and the system which we investigate in this section appears in the coefficient of the β-function. Namely, the coefficient factor α_0 of the running coupling in eq. (4.1) is taken to be

$$\alpha_0 = \frac{4\pi}{\beta_0} = \frac{12\pi}{11N_c - 4N_D} \ , \tag{5.8}$$

where β_0 is the coefficient of one-loop β-function. For the small value of β_0 the coupling runs very slowly, and the system well simulates the walking technicolor model[15].

Using the same procedure as the previous one for real QCD, we evaluate S parameter and the pion decay constant with $N_D = 1, \cdots, 6$. The results are shown in Table 5. We find that the dominant support (cf. Fig. 3) lies on the energy region

N_D	1	2	3	4	5	6
S/N_D	0.469	0.457	0.442	0.431	0.430	0.421
$(f_\pi/\Lambda_{\rm QCD})^2/N_D \times 100$	3.87	4.27	4.87	6.05	9.32	24.7
$\Lambda_{\rm QCD}$ [MeV]	473	318	243	189	136	76.4

Table 5: The values of S/N_D and $f_\pi/\Lambda_{\rm QCD}$ for the number of doublets $N_D = 1, \cdots, 6$ with $t_F = 0.5$ fixed. We also show the values of $\Lambda_{\rm QCD}$ by imposing $f_\pi = 93$ MeV.

higher for large N_D than for small N_D. The values of $\Lambda_{\rm QCD}$ become small for large number of doublets. However, we cannot see the clear dependence on N_D of the values of S/N_D. The value slightly decreases as N_D increased, only by 11%. Our result shows that S parameter almost scales linearly with N_D, which supports the naive estimation by Refs. [3, 24].

Finally we check the dependence on the infrared cutoff t_F with $N_D = 5$, and show the results in Table 6. The dependence on the infrared cutoff t_F of $\Lambda_{\rm QCD}$ should be compared with the result in the case of single-sextet quark in Ref. [10]. They calculate $f_\pi/\Lambda_{\rm QCD}$ using the homogeneous BS equation of pion, and find that the slowly running coupling gives stable results less dependent on t_F. Our results conform to theirs.

Acknowledgements

t_F	0.3	0.5	0.7	0.9	1.1
S/N_D	0.450	0.430	0.432	0.436	0.446
$(f_\pi/\Lambda_{\rm QCD})^2/N_D \times 100$	8.82	9.32	9.78	10.2	10.4
$\Lambda_{\rm QCD}$ [MeV]	140	136	133	130	129

Table 6: The dependence on the infrared cutoff t_F for $N_D = 5$.

We would like to thank T. Kugo for useful discussions and comments. M.H. is supported in part by the Grant-in-Aid for Scientific Research (#2208) from the Ministry of Education, Science and Culture.

References

[1] J. Gasser and H. Leutwyler, Ann. Phys. (N.Y.) **158**, 142 (1984); Nucl. Phys. **B250**, 465 (1985).

[2] B. Holdom and J. Terning, Phys. Lett. **B247**, 88 (1990).

[3] M. Peskin and T. Takeuchi, Phys. Rev. Lett. **65**, 964 (1990).

[4] G. Altarelli and R. Barbieri, Phys. Lett. **B253**, 161 (1991).

[5] J.F. Donoghue, C. Ramirez and G. Valencia, Phys. Rev. **D39**, 1947 (1989); G. Ecker, J. Gasser, H. Leutwyler, A. Pich and E. de Rafael, Phys. Lett. **B233**, 425 (1989).

[6] B. Holdom, J. Terning and K. Verbeek, Phys. Lett. **B245**, 612 (1990).

[7] B. Holdom, Phys. Rev. **D45**, 2534 (1992).

[8] J.F. Donoghue and B. Holstein, Phys. Rev. **D46**, 4076 (1992).

[9] S. Weinberg, Phys. Rev. Lett. **18**, 507 (1967).

[10] K-I. Aoki, M. Bando, T. Kugo and M.G. Mitchard H. Nakatani, Phys. Lett. **B266**, 467 (1991).

[11] K. Higashijima, Phys. Rev. **D29**, 1228 (1984).

[12] V. Miransky, Sov. J. Nucl. Phys. **38**, 280 (1984).

[13] P. Jain and H.J. Munczek, Phys. Rev. **D44**, 1873 (1991).

[14] K-I. Aoki, T. Kugo and M.G. Mitchard, Phys. Lett. **B266**, 467 (1991).

[15] B. Holdom, Phys. Lett. **B150**, 301 (1985); K. Yamawaki, M. Bando and K. Matumoto, Phys. Rev. Lett. **56**, 1335 (1986); T. Akiba and T. Yanagida, Phys. Lett. **B169**, 432 (1986); T. Appelquist, D. Karabali and L.C.R. Wijewardhana, Phys. Rev. Lett. **57**, 957 (1986).

[16] T. Appelquist and G. Triantaphyllou, Phys. Lett. **B278**, 345 (1992).

[17] T. Das, V. Mathur and S. Okubo, Phys. Rev. Lett. **19**, 859 (1967).

[18] T. Inami, C.S. Lim and A. Yamada, Mod. Phys. Lett. **7**, 2789 (1992).

[19] T. Kugo, M.G. Mitchard and Y. Yoshida, Prog. Theor. Phys. **91**, 521 (1994).

[20] J. Bijnens, C. Bruno and E. de Rafael, Nucl. Phys. **B390**, 501 (1993).

[21] M.A. Shifman, A.I. Vainshtein and V.I. Zakharov, Nucl. Phys. **B147**, 385 (1979).

[22] T. Kugo and M.G. Mitchard, Phys. Lett. **B286**, 355 (1992).

[23] The experimental value of the ρ meson mass is given in
Particle Data Group: Review of Particle Properties, Phys. Rev. **D45**, (1992);
and the decay constant is given in
J. Gasser and H. Leutwyler, Phys. Rep. **87**, 77 (1982).

[24] T. Takeuchi, in *Proc. of International Workshop on Electroweak Symmetry Breaking*, Nov. 12-15, 1991, ed. W.A. Bardeen, J. Kodaira and T. Muta (World Scientific Pub. Co., Singapore, 1991), p. 165.